

THREE-DIMENSIONAL FLOW SEPARATIONS IN THE DIFFUSER OF A STEAM TURBINE CONTROL VALVE

Manuel B. Clari
Power Engineering
Laboratory for Turbomachinery
Helmut Schmidt University
University of Federal Armed
Forces Germany Hamburg
Holstenhofweg 85
D-22043 Hamburg, Germany
E-mail: mclari@hsu-hh.de

Thomas Polklas
MAN Diesel & Turbo SE
Steinbrinkstr. 1
46145 Oberhausen
Germany
E-mail: thomas.polklas@man.eu

Franz Joos
Power Engineering
Laboratory for Turbomachinery
Helmut Schmidt University
University of Federal Armed
Forces Germany Hamburg
Holstenhofweg 85
D-22043 Hamburg, Germany
E-mail: joos@hsu-hh.de

ABSTRACT

A test rig for Steam Turbine Control Valves is operated at the Laboratory of Turbomachinery of the Helmut-Schmidt-University in Hamburg. The control valve unit containing four independently operable valves is a mockup of a typical steam turbine design converted for the use of compressed air with a maximum of 4 bar. The investigations focus on the transient flow behavior and fluid-structure interaction in connection to valve lift and pressure ratio.

Validated by the pressure measurements, transient CFD simulations have been conducted identifying the flow separation structures and the transient behavior of the flow inside the valve throat and diffuser in detail.

Similar to published separation structures in compressor cascades the transonic flow inside the valve shows three-dimensional flow separation structures and vortices which can be identified by the two-dimensional streamlines on a plane with a constant and infinitesimal distance to the wall. Furthermore a transient development of these patterns can be identified.

INTRODUCTION

Similar to the development of steam turbines for power generation with fossil or nuclear fuels, the development in the industrial steam turbine designs for the low to medium power outputs for decentralized purposes or combined cycle power plants lead to higher steam chest temperatures and pressures. These steam conditions are still considerable lower than typical conditions appearing in bigger steam turbines for power generation. To allow a wider range of performance which is typical for those design of turbines a more complex mechanism of controlling the mass flow through the steam turbine is

necessary. Hardin et al. [1], Zhang et al. [2], [3], Deich et al. [4] or Tecza et al. [5] point out that the common lift bar design for steam turbines (fig. 1) with governing nozzle groups are prone to oscillating flows in the valve diffuser of the steam control valve at critical operation conditions with critical frequencies of the pressure pulsations from 230 – 350 Hz or up to 1600 Hz depending on the reference. The oscillating flow at certain operation condition amplifies through interaction with the valve structure by bending and rotating the plug and stem. This could lead to failure of the plug or stem and damage the steam control valve. To reduce or prevent fluid structure interaction an alternative control valve design is needed, which protects the control mechanism from the steam flow in the steam chest and trough the valve.

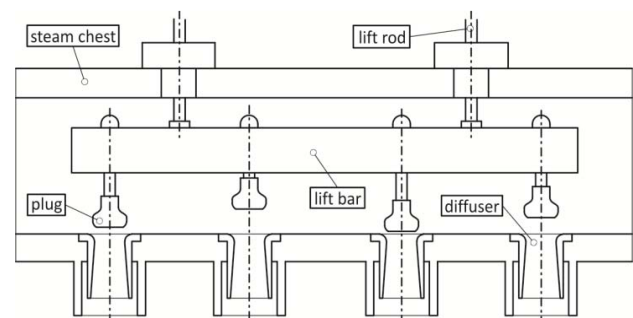


FIGURE 1. LIFT BAR DESIGN WITH 4 VALVES

A new valve design (s. fig. 2) was built as test rig to measure the flow conditions at different operation conditions. It features single operable valves with the valve stem and plug moving within a bushing. Thus protecting the stem and plug

from the flow in the steam chest as well as preventing a flow induced bending or rotation of the plug. The nature of the valve flow includes unstable flow separation as well as transonic flow. Due to limited space to apply sensors or mount windows for optical flow measurement systems, not only measured data will be used to analyze this new valve design. The measured data will provide a basis for CFD simulations to further investigate the flow in the valve and get detailed information of the mechanisms of the valve flow. Since the flow separation in the valve diffuser is the main reason for an unstable valve flow a method to analyze the flow separation with the CFD simulation is introduced. The main objective is to prove that the new design tends less to fluid structure interaction and is less prone to critical operation conditions.

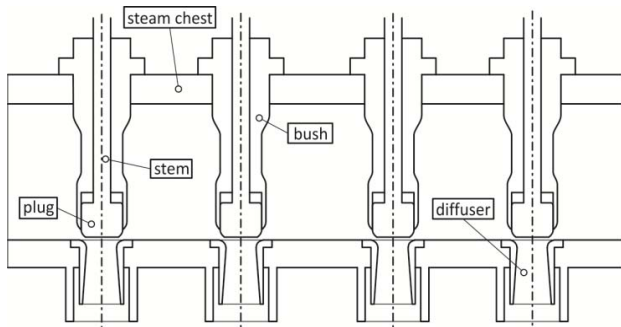


FIGURE 2. SINGLE OPERABLE VALVE DESIGN USED IN THE TEST RIG

NOMENCLATURE

- a normalized axial length
- b distance of plane to wall
- c flow velocity
- d diameter
- f frequency of pressure oscillation
- l lift
- OR opening ratio l / d
- p static pressure
- PR static pressure ratio p / p_{sc}
- t temperature
- u velocity component in plane corresponding to surface
- v velocity component in plane corresponding to surface
- x coordinate in the plane corresponding to surface
- y coordinate in the plane corresponding to surface

Greek Symbols

- α polar angle

Subscripts

- v valve
- air air
- amb ambient
- sc steam chest of the control valve
- steam steam
- in steam chest inlet

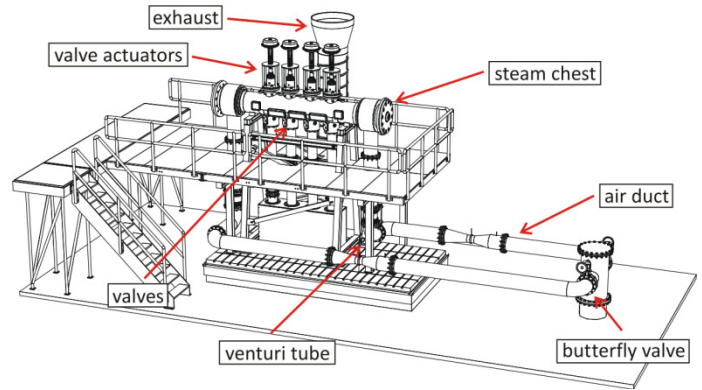


FIGURE 3. ISOMETRIC VIEW OF THE TEST RIG

EXPERIMENTAL SET UP

The test rig set up is shown in fig. 3. Its main component is a steam turbine control valve, with a design deduced from a commercial design. The four valves mounted within the steam chest can be operated separately. Each valve consists of an immobile diffuser mounted in the steam chest and a moving plug attached on the end of a stem. The moving valve part (plug and stem) are placed within a protective bushing. This bushing acts as guidance for the translational movement and protection from the flow. Four different valve sizes were investigated, characterized by the narrowest diffuser diameter d_v ranging from 80 to 140 mm. The valves are placed inside the steam chest as depicted in fig. 2. The pressurized air for the experiments is supplied through two air ducts leading to either side of the steam chest in the following regarded as valve 1 side or valve 4 side of the steam chest (fig. 4). Each duct can be closed with a butterfly valve allowing the variation of flow to the steam chest. Downstream of each valve a duct directs the flow into the ambience. To measure the massflow through the test rig venturi tubes are located in each duct leading to the steam chest. To evaluate the massflow through each valve replaceable orifices were used in the ducts behind the valves. The test rig is constructed for air at a pressure $p_{sc} < 4$ bar and a temperature $t_{sc} < 40^\circ\text{C}$.

The operation conditions of the test rig can be compared with the operation conditions of the typical steam turbine design ($p_{sc} = 140$ bar, $t_{sc} = 540^\circ\text{C}$) through the similitude of Mach, Reynolds and Strouhal number. First the Mach number range of the test rig should reproduce that Mach number range of a steam turbine, deriving the mass flow needed to operate the test rig. The Reynolds number represents the character of the flow. For both cases a high Reynolds number ($Re > 5 \cdot 10^6$) indicates a turbulent flow. Finally the Strouhal number characterizes the separation behavior and is a function of the Reynolds number. It is about $Sr = 0.2$ for both, steam and air. Evaluating the Strouhal number shows that frequency of flow separation and pulsation with air and the test conditions should be about $f_{air} = 0.585 \dots 0.6 f_{steam}$.

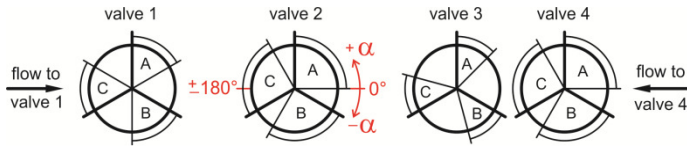


FIGURE 4. VALVE POSITIONS AND SENSOR GROUPS A, B AND C AT DIFFUSER

SENSORS

Depending on the diffuser size 21 or 36 piezoresistive pressure transducers are located on the stationary side of the valve throat and the following diffuser section. The pressure transducers are grouped circumferentially into three rows A, B and C. The smaller valves 3 and 4 only have sensors 1 – 7 and the valves 1 and 2 have additional sensors 8 – 12 per row (fig. 5).

Due to limited space in the transition section to the diffuser the transducers couldn't be mounted aligned in a row in stream direction. Instead they are positioned with a circumferential displacement (fig. 4). Depending on the valve size this displacement varies from 45° to 90° for a single row of pressure sensors.

The measurement equipment allows sampling rates up to 2400 Hz for maximal 36 pressure transducers to a maximum of 4 bar at an accuracy of 0.5 % or 20 mbar.

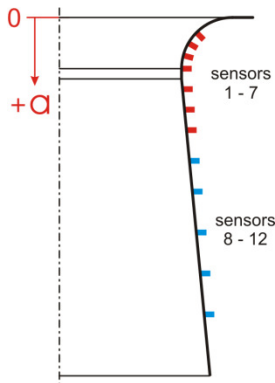


FIGURE 5. AXIAL POSITION OF PRESSURE SENSORS

EXPERIMENTS

The experiments conducted concentrate on valve 1 and 2 with variation in lift and pressure ratio. Only steady operation points in respect to lift and pressure ratio will be presented in this paper with the incident flow to the steam chest coming from the steam chest side where valve 1 is located. Therefore an estimate can be given at which steady operation condition unsteady flow in the valve occurs. Valve 1 was measured at about 215 operation points with an opening ratio up to $OR = 0.41$ and the static pressure ratio (pressure after the valve normalized with the steam chest pressure) ranging from $PR = 0.52$ to $PR = 0.83$. For valve 2 over 40 operation points were investigated with the maximal $OR = 0.21$ and a $PR = 0.52 \dots 0.83$ measured. About 120 signal samples with a length of 1s were recorded at every sensor and operation point.

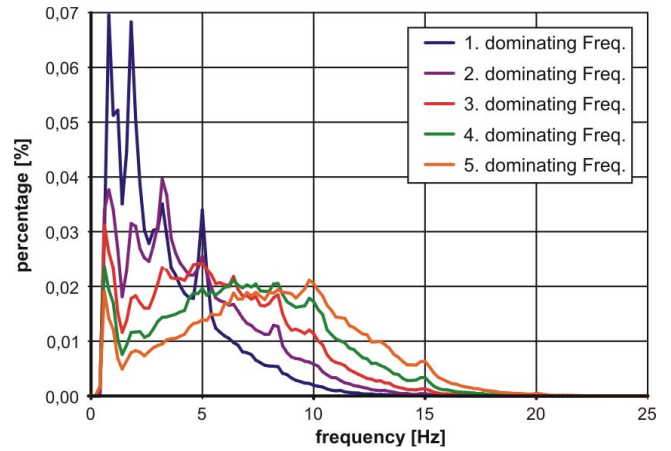


FIGURE 6. HISTOGRAM OF DOMINATING FREQUENCIES FOR ALL MEASURED SAMPLES (VALVE 1)

RESULTS

The dominating frequency of a measured pressure signal can be evaluated with a time resolved FFT-spectrum. Evaluating the FFT-spectrum for all sensors at different operation conditions shows no high frequency. This can be depicted by combining all dominating frequencies of all measured samples for all operation points to produce the histograms shown in fig. 6 for valve 1 and fig. 7 for valve 2. This emphasizes that at no operation point the domination frequency exceeds 15 Hz for both valves tested. A closer look shows that the frequency of pressure pulsations exceeds 5 Hz in about 20% of the measurements and 10 Hz in about only 1.5%. The arithmetic mean of the dominating frequency is about 3.4 Hz for valve 1 and 3.6 Hz for valve 2. Furthermore a peak at 5.0 Hz can be found for valve 1. This corresponds to the idle frequency of the pressure sensors. Furthermore it indicates that in about 3% of the measurements the pressure fluctuations were smaller than the accuracy of the sensors. It can be stated that for no operation condition a critical flow pulsation occurred.

Transferring these results by the laws of similitude to the test conditions described by Hardin and Kushner [1] ($p_{sc} \approx 114$ bar, $t_{sc} \approx 460^\circ\text{C}$) a factor of about 1.6 (1.583 .. 1.624) applies on the frequencies described above. This corrects the average frequency to about 5.75 Hz. This differs significantly from the results reported in the literature with high pressure amplitudes at 30 – 40 Hz and about 350 Hz at low lifts and high pressure ratios for a steam turbine with a lift bar control valve design.

The significant difference in frequency is a result of the more sturdy design of the valve stem, plug and the protective bushing which prevents the bending and rotation of the plug and stem. Therefore the fluid-structure interaction can be damped and no amplification of the pressure will occur.

By analyzing a recorded signal it can be stated either the flow is attached or separated as following example illustrates:

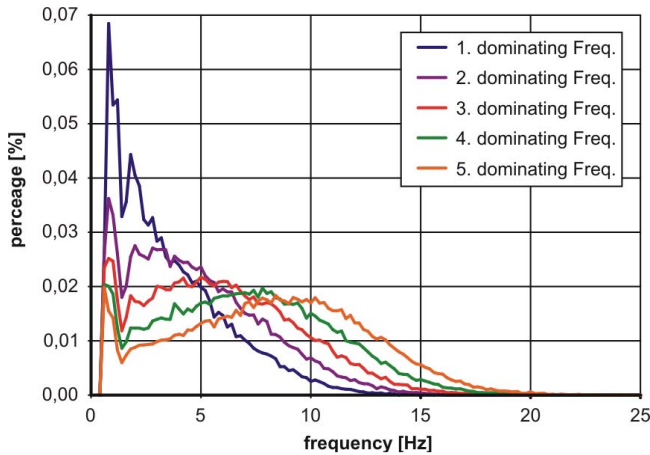


FIGURE 7. HISTOGRAM OF DOMINATING FREQUENCIES FOR ALL MEASURED SAMPLES (VALVE 2)

Figure 8 shows two graphs for an attached diffuser flow (red) and a separated flow (green). The thick lines depict the mean pressure ratio normalized with the steam chest pressure. The thin lines show the minimum respectively maximum of the recorded pressure signal. If the flow is attached to the wall the sensors show a slight rising pressure in downstream direction. A separated flow at the sensors will show nearly constant pressure after the flow separated. In general the sensors in the lower diffuser section show a lower local static pressure ratio (pressure at sensor normalized with the steam chest pressure) if the flow is separated from the wall then the attached flow. The approximate position of the limiting cross section for the attached flow in the valve throat is indicated by the lowest pressure, which corresponds to the highest velocity in the limiting cross section.

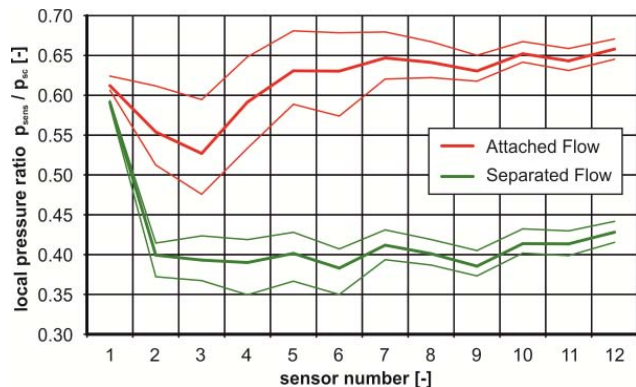


FIGURE 8. NORMALIZED PRESSURE RATIOS FOR A ATTACHED AND SEPARATED DIFFUSER FLOW

Single peaks in the pressure signals may occur at certain operating conditions and are measured for every downstream sensor after the throat cross section of the valve. These peaks may occur for all sensor rows at the same time and only vary in amplitude. This indicates that the short flow change affects the

whole valve at an instant. This is an evidence for an instable flow without a vortex or circumferential fluctuation.

Varying the side of the incident flow from the side of valve 1 to the side of valve 4 (fig. 4) seems to have no significant influence on frequency or amplitude of the wall pressure.

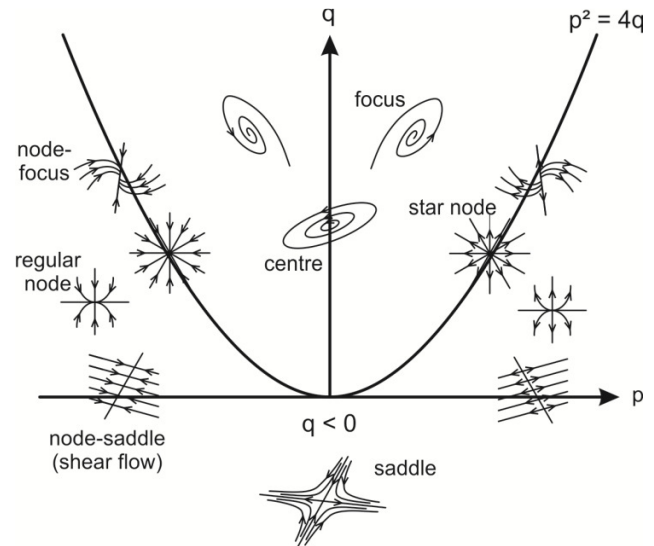


FIGURE 9. CLASSIFICATION OF CRITICAL POINTS OF TWO-DIMENSIONAL STREAMLINES (DALLMANN [6])

SEPARATION BEHAVIOR

To evaluate the valve flow the knowledge about three-dimensional flow separations and transient behavior of the flow is necessary. By constructing two-dimensional streamlines of the three-dimensional flow within a plane close to the wall different types of critical points and the corresponding streamline pattern can be visualized. These patterns were published by Dallmann [6] and are displayed in fig. 9. The Critical points can be distinguished by the trace p and the determinant q of the Jacobian matrix of the two-dimensional velocity components.

$$p = \frac{\delta u}{\delta x} + \frac{\delta v}{\delta y}$$

$$q = \frac{\delta u}{\delta x} \frac{\delta v}{\delta y} - \frac{\delta u}{\delta y} \frac{\delta v}{\delta x}$$

For $p > 0$ the critical points corresponds to an attaching flow. On the other hand the flow separates if the trace is $p < 0$. This is visualized by the streamlines gathering at the critical point if the flow separates from the wall and diverting from it if the flow attaches.

Tobak and Peak [7] and Perry and Chong [8] point out that the patterns which meet one of the following conditions are unstable. If either the trace p or the determinant q is 0. This includes a node-saddle or centre node. All critical points on the

parabola $p^2 = 4q$ (node-focus and star node) are unstable as well. The remaining points (saddle point, regular node, focus) are the only stable patterns.

Gdadebo [9] uses this method to construct and evaluate the separation behavior of compressor cascades. As a result Gdadebo states the index rule as a criterion for a stable flow in compressor cascade.

This approach will be used in the following analysis of transient CFD simulations of the flow in the steam chest and trough the valve, focusing on the valve diffuser for this is the central component where the critical flow conditions may occur. Contrary to Gdadebo not only stable patterns will be examined. Especially the evolving and dissolving of transient respectively unstable two-dimensional patterns are at the centre of interest.

CFD SIMULATIONS

As stated above the measurements indicate an inhomogeneous flow to the valve throat. Thus the geometric boundaries for a CFD simulation can't be set near the valve throat. Instead the whole steam chest with all four valves including the bushings and plugs are modeled. The boundary conditions were set according to the measured operation conditions. Two simulations for valve 2 at an opening ratio $OR = 0.15$ and pressure ratios of $PR = 0.708$ and $PR = 0.524$ were simulated.

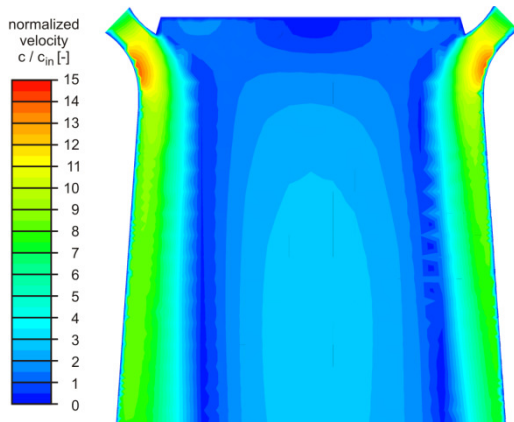


FIGURE 10. PRESSURE PLOT SINGLE CFD TIMESTEP (VALVE 2, $PR = 0.708$)

ANSYS CFX 12.0 is used as CFD solver. A tetrahedral mesh was used with a resolution of about 4.5 million elements for the steam chest and about 2.4 million for the valve. This allows a y^+ of 100 to 400 within the valve throat and a y^+ of 5 to 90 at the diffuser wall. The shear stress transport model is used as turbulence model. The convergence criterion is an overall residual below 10^{-4} for each timestep. The transient solution is calculated with a timestep of $2 \cdot 10^{-4}$ s.

As example a single timestep of transient CFD results of the first case is displayed in fig. 10 as the cross section through to valve. The flow is attached on the whole circumference of

the diffuser forming an annular jet. The narrowest valve cross section hasn't choked at this pressure ratio.

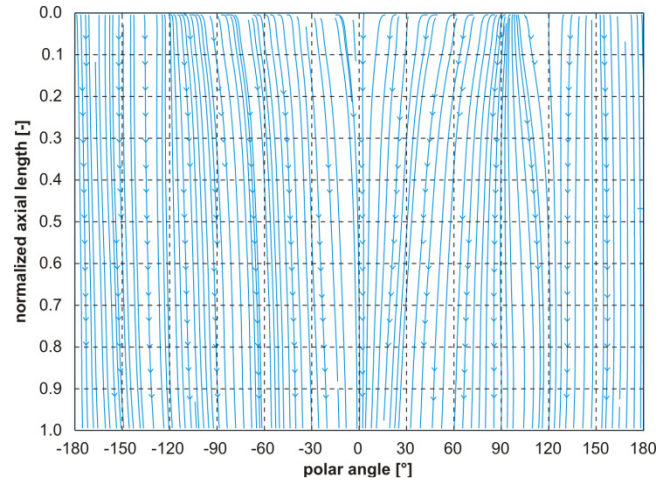


FIGURE 11. TWO-DIMENSIONAL STREAMLINES NEAR THE DIFFUSER WALL FOR SAME TIMESTEP AS FIG. 10 (VALVE 2, $PR = 0.708$, $b = 0.05$ mm)

The corresponding two-dimensional streamlines are depicted in fig. 11 were the plane of interest with a distance of $b = 0.5$ mm from the wall is unreeled to produce that diagram. The x-axis represents the polar angle α as depicted in fig. 4. The y-axis shows the axial length a along the diffuser axis normalized by the diffuser length (fig. 5). The streamlines flow downstream with only a small velocity component perpendicular to the main flow direction and little change over time. The annular flow attaches at the whole circumference of the valve diffuser and forms a stable flow without any separations.

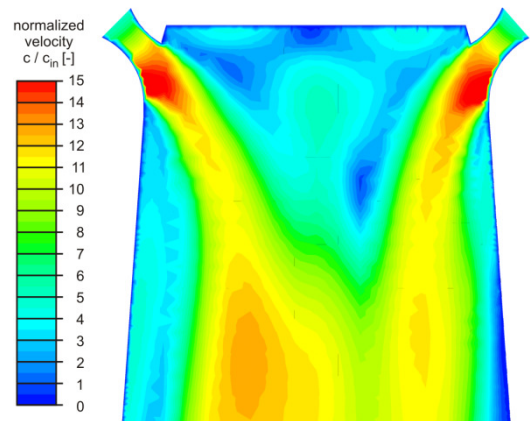


FIGURE 12. PRESSURE PLOT SINGLE CFD TIMESTEP (VALVE 2, $PR = 0.524$)

For the higher steam chest pressure a single timestep of the CFD simulation is depicted in fig. 12. The valve is choked and the annular valve cross section works as a Laval nozzle. The

supersonic flow can't follow the surface of the valve and lifts off the wall near the end of the transitional radius resulting in a shock slowing the velocity to subsonic speeds. The free jet merges near the valve axis to an unstable jet attaching and separating further downstream from the wall.

Similar to the first case the two-dimensional streamlines in a plane ($b = 0.5 \text{ mm}$) corresponding to the surface were calculated (fig. 13). The separation of the supersonic flow from the wall caused by the shock can be found at the top of the diagram at about $a = 0.1$. This separation is limited in its movement due to shock-separation interaction. The vortices forming within the annular separation bubble around the free jet in the centre can be visualized by the method described earlier.

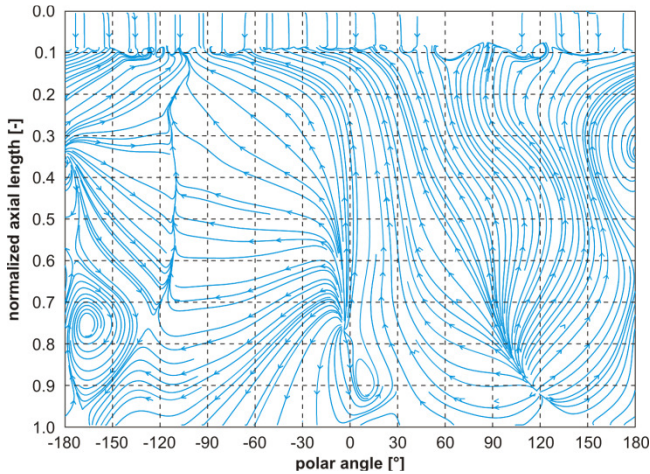


FIGURE 13. TWO-DIMENSIONAL STREAMLINES NEAR THE DIFFUSER WALL FOR SAME TIMESTEP AS FIG. 12 (VALVE 2, $PR = 0.524$, $b = 0.05 \text{ mm}$)

In this example nine critical points (four saddle points, three focus points, two regular nodes) in the separation area can be found. Together these critical points form different streamline patterns. Some of these critical points occur frequently and seem to both form and dissolve the same way each time they happen. This means the three-dimensional flow has a certain regular basis. Mapping the p and q values of the flow is not possible at this moment due to the complex geometry that must be unreel to a perpendicular coordinate system.

VALIDATION

Figure 14 depicts the normalized static pressure ratios over the sensor number for the second CFD simulation at a $PR = 0.524$ (s. fig. 12/13). The green lines represent the measured data and the red lines the simulated data normalized with the steam chest pressure. As in fig. 8 the thick lines depict the average value and the thin line the minimal respectively the maximal value. Comparing the graphs two separate sections can be identified. Beginning with sensor 5 downstream the simulated data fits the measured data with a slight higher fluctuation. Thus the flow in separation area corresponds to the measurements.

For the sensors 1 to 4 the simulated data shows a distinct deviation to the measured data. This indicates a higher acceleration of the flow in the valve throat. Since the separation area downstream of the shock (between sensor 4 and 5) is the area of interest for the following qualitative illustration the CFD simulation will suffice. To make a quantitative statement an improved CFD would be necessary.

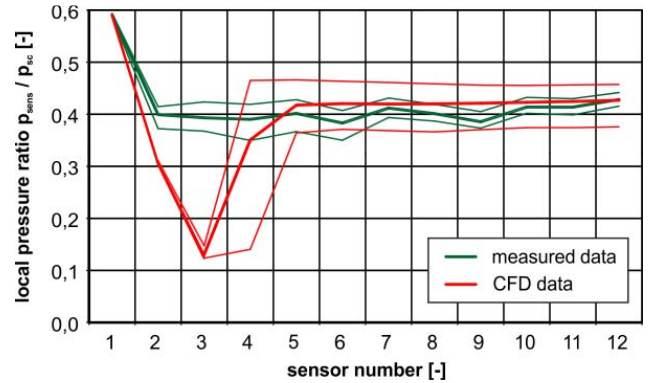


FIGURE 14. NORMALIZED PRESSURE RATIOS FOR MEASURED AND SIMULATED VALVE 2 ($PR = 0.524$)

FLOW PATTERN

Analyzing the three-dimensional flow of the example above (fig. 13) three main patterns will be explained in detail. The first noticeable pattern is a separation line running from a saddle point $a = 0.75$ and $\alpha = -120^\circ$ versus the main flow direction back to the separation line due to the shock at $a = 0.1$. Figure 15 shows the two-dimensional streamlines on the left and the three-dimensional streamlines running through this separation area on the right.

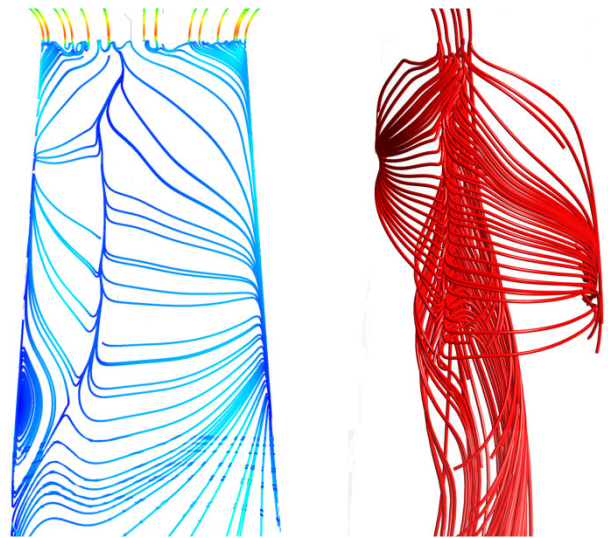


FIGURE 15. TWO AND THREE-DIMENSIONAL FLOW PATTERN 1 – VIEW $\alpha = -90^\circ$ (VALVE 2, $PR = 0.524$, $b = 0.05 \text{ mm}$)

In the two-dimensional pattern the streamlines converge to a single streamline. This means the flow streams from either side meet at that specific streamline and lift off the wall. Corresponding to that, the three-dimensional streamlines coming from each circumferential direction merge to single stream at this location. Indicated by the two-dimensional streamline the mixed flow streams upstream and merges with the supersonic jet flow near the shock. This pattern seems to have a significant role for it builds a barrier between different areas in the separation bubble.

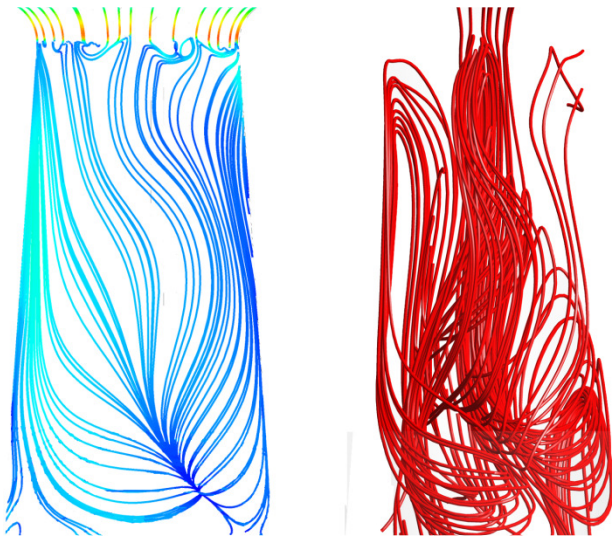


FIGURE 16. TWO AND THREE-DIMENSIONAL FLOW PATTERN 2 – VIEW $\alpha = 90^\circ$ (VALVE 2, PR = 0.524, b = 0.05 mm)

The next critical points are two regular nodes at $a = 0.85$, $\alpha = 105^\circ$ as well as at $a = 0.75$, $\alpha = 0^\circ$ (fig. 13). Only the first point is depicted in fig. 16 for the three-dimensional flow forming both critical points is similar. Again the two-dimensional streamlines are shown on the left and the three-dimensional streamlines on the right. This pattern is formed by a part of the jet flow attaching near the end of the diffuser. The attaching flow diverts in all directions away from the attaching point. The main direction is upstream into the separation bubble where the flow circulates until it is transported downstream with the main flow. A part of the attaching flow streams to the side in circumferential direction. The depicted regular node generates a flow that forms pattern 3 (s. below), while the regular node at $a = 0.75$ mm and $\alpha = 0^\circ$ forms a part of the flow that result in the separation line described in pattern 1.

The last pattern 3 is displayed in fig. 17. This pattern consists of three critical points and is influenced by both patterns described above. A saddle point marks the centre (fig. 11, $a = 0.55$, $\alpha = -175^\circ$) and on each side the separation line of the saddle point curls up into a focus node respectively centre point. The three-dimensional flow shows the focus-node streamlines in blue and the streamlines forming the centre point colored in red. The streamlines indicate that both vortices come

from the same valve throat section. The flow is following the jet stream to the end of the diffuser section where they attach as explained for fig. 15. Therefore both vortices are a result of the attaching flow coming from the regular node at $a = 0.85$ and $\alpha = 105^\circ$. While the red streamlines split up and flow in circumferential direction, the blue streamlines travel further upstream until they are redirected in circumferential direction as they reach the shock induced separation. Both streams flow towards the separation line explained as pattern 1 (fig. 15), while the blue flow separates from the wall at this separation line mixing with the flow from the regular node at $a = 0.75$ and $\alpha = 0^\circ$. The red stream is deflected and forms a vortex which only can separate from the wall and flow downstream towards the diffuser outlet.

These patterns are unstable and change with time. They form a system of interacting vortices within the separation bubble. Also they influence the free supersonic jet and vice versa are influenced by the jet. Examining these complex three-dimensional flows can be simplified by a time series of diagrams depicting the two-dimensional streamlines as explained above. The research on the development of the two-dimensional pattern over time leads to a better understanding of the transient three-dimensional flow.

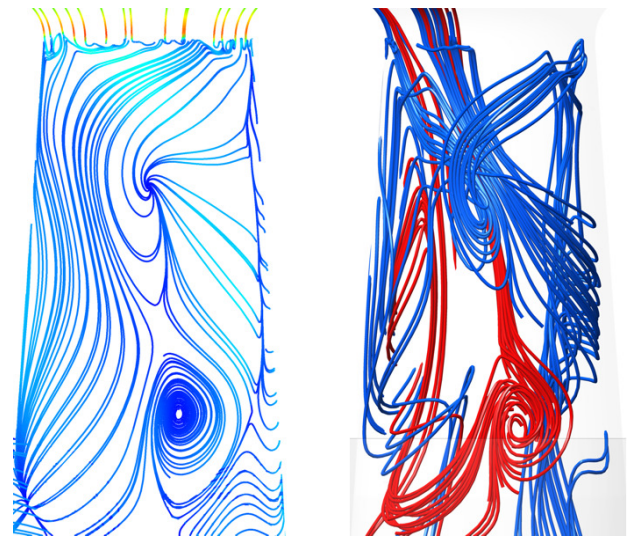


FIGURE 17. TWO AND THREE-DIMENSIONAL FLOW PATTERN 3 – VIEW $\alpha = -180^\circ$ (VALVE 2, PR = 0.524, b = 0.05 mm)

CONCLUSION

The experiments show different results from other published research as [1], [2], [3], [4] and [5]. The main difference is the frequency of flow separation. While the references offer measurements with steam as fluid and frequencies of the pressure instabilities from 230 – 350 Hz or up to 1600 Hz, the presented measurements with air only show pressure pulsations around 3.5 Hz. Transferred by the laws of similitude this correlates to a frequency of 5.75 Hz with steam as fluid. It appears that the different design which replaces the

exposed lift bar design by single operable valves mounted in protective bushings reduces fluid-structure interaction.

Based on CFD simulations a method to evaluate the separation behavior of the valve flow was introduced. This method was used to illustrate the three-dimensional flow through the valve and the valve diffuser by two-dimensional streamlines in a plane close to the wall of the diffuser.

FUTURE ASPECTS

The future research will focus on the following aspects. First: Detailed analysis of the difference in the frequency of flow separation between a lift bar design and a single valve design. Second: Conducting measurements during the opening or closing movement of each single valve and analyzing if critical amplification of the pressure pulsations may occur. Third: Transient CFD simulation with higher resolution will be conducted to identify connections of operation conditions and three-dimensional flow structures. In addition the forming and break-up of unstable flow structures will be evaluated. Another object will be a catalogue of typical patterns and their characteristics as well as mapping the p and q values of the flow.

ACKNOWLEDGMENTS

The authors gratefully acknowledge MAN Diesel & Turbo SE for their support and permission to publish this paper. The responsibility for the content lies solely with its authors.

REFERENCES

- [1] Hardin J., Kushner F., Koester S., 2003, Elimination of flow-induced Instability from Steam Turbine Control Valves, Proc. of the 32nd Turbomachinery Symposium, pp 99-108
- [2] Zhang D., Engeda A., 2003, Venturi Valves for Steam Turbines and Improved Design Considerations, Proceedings Institution of Mechanical Engineers Vol. 217 Part A, pp. 219-230
- [3] Zhang D., Engeda A., Hardin J.R., Aungier R.H., 2004, Experimental Study of Steam Turbine Control Valves, Proceedings Institution of Mechanical Engineers Vol. 218 Part C, pp. 493-507
- [4] Deich M.E., Sapunov O.G., Shanin V.K., 1979, Flow of Superheated and Wet Steam in Governor Valves of Steam Turbines, Thermal Engineering 26 (4), pp. 215-218
- [5] Tecza J., Chochua G., Moll R., 2010, Analysis of Fluid-Structure Interaction in a Steam Turbine Throttle Valve, ASME Paper GT2010-23788, pp. 1-10
- [6] Dallmann U., 1983, Topological Structures of Three-dimensional Flow Separation, DFVLR, IB 221-82-A07, Göttingen, Germany
- [7] Tobak M., Peak D.J., 1982, Topology of Three-dimensional Separated Flows, Annual Review of Fluid Mechanics Vol. 14, pp. 61-85
- [8] Perry A.E., Chong M.S., 1987, A Description of Eddying Motions and Flow Patterns using Critical Point Concepts, Annual Review of Fluid Mechanics Vol. 19, pp. 125-155
- [9] Gbadebo S. A., Cumpsty N. A., Hynes T. P., 2004, Three-dimensional Separations in Axial Compressors, ASME Paper GT2004-53617, pp. 1-13